Terahertz birefringence and attenuation properties of wood and paper

Matthew Reid and R. Fedosejevs

Department of Electrical and Computer Engineering, University of Alberta, Edmonton, Canada

The far-infrared properties of spruce wood are examined using a terahertz time-domain spectrometer. The solid wood is shown to exhibit both birefringence and diattenuation. The birefringence properties are sufficient to construct a quarter waveplate, operating at 0.36 THz, and a half waveplate operating at 0.71THz. The origin of the birefringence is attributed to the preferential fibre orientation within the wood. Similar birefringence is observed in lens paper where the fibres are preferentially oriented in one direction.

OCIS codes: 230.5440,160.4890,160.4760

1. Introduction

Many materials are transparent in the far infrared making it an interesting diagnostic wavelength range for material inspection. The fact that the far-infrared radiation, at the levels typically present in a terahertz time-domain spectrometer, pose no significant health hazard[1] make it attractive for many application areas such as in imaging[2] and security.[3,4]

It has been recognized early on that there may be applications to the wood industry for pulsed terahertz radiation.[5,6] This is primarily due to the fact that pulsed terahertz radiation offers access to a frequency range of transparency in wood. In the work of Koch et. al.,[5] it was demonstrated that transmission imaging of wood could be performed with a resolution sufficient to distinguish annular rings using a terahertz time-domain spectrometer. However, there has been little work since these early investigations.

In this report, the far-infrared properties of common spruce wood are studied in detail, and it is demonstrated that the wood exhibits both diattenuation and birefringence. These properties are demonstrated by constructing a waveplate from wood, and also demonstrate the potential for fibre orientation analysis with pulsed terahertz radiation.

Fibre orientation analysis has traditionally relied upon methods involving optical scattering measurements,[7] X-ray diffraction measurements[8,9] and the use of fibre dyes.[10] The electromagnetic methods for the determination of fibre orientation rely on the structure of the cellulose, which makes up the fibre.[7–10]

In the present report, we present an alternative approach to measuring fibre orientation using far-infrared radiation, and the polarizing properties of the fibres. This method has the advantage that it can be operated in a transmission mode for samples up to the order of 1 cm in thickness, for which optical techniques cannot. Moreover, it also has the advantage that X-rays are not required, and the radiation used is non-ionizing and safe.[1]

2. Experimental

The experimental set-up used is shown in Fig. 1, and similar to that reported previously.[11] A semi-large aperture photo-conductive switch[12] is used as a source of terahertz radiation. The switch is formed using silver paint on a SI-GaAs substrate, with a minimum separation of $470\mu m$, biased with a 250 V peak, 40 kHz sine wave. The switch is driven with 300 mW of optical power from an 80 MHz, 100 fs, Ti:Sapphire oscillator. The optical beam is split into pump and probe beams. The pump is lightly focused on the photoconductive switch, and the emitted terahertz radiation which is horizontally polarized is imaged onto a 1 mm thick (110) oriented ZnTe crystal which is used to detect the radiation via the linear electro-optic effect,[13] using 4 F/2, 2" diameter, 90^o off-axis parabolic mirrors. The four mirrors form an intermediate focal plane, in which the samples are placed for the studies that follow.

Polarization sensitive measurements are made, where the ZnTe crystal is used as a polarization analyzer for the terahertz radiation.[13] The probe beam is linearly horizontally polarized, and the orientation of the [001] axis of the ZnTe crystal is oriented to either detect vertically, or horizontally polarized terahertz radiation at the detector.

Two samples of solid spruce wood, with thicknesses of 8.3 mm and 3.025 mm were studied. The samples were purchased from a hardware store and cut to the desired size, and given a smooth finish. The samples were exposed to air, and therefore subjected to ambient humidity. The lens paper investigated in this report was standard lens paper purchased from Fisher Scientific.

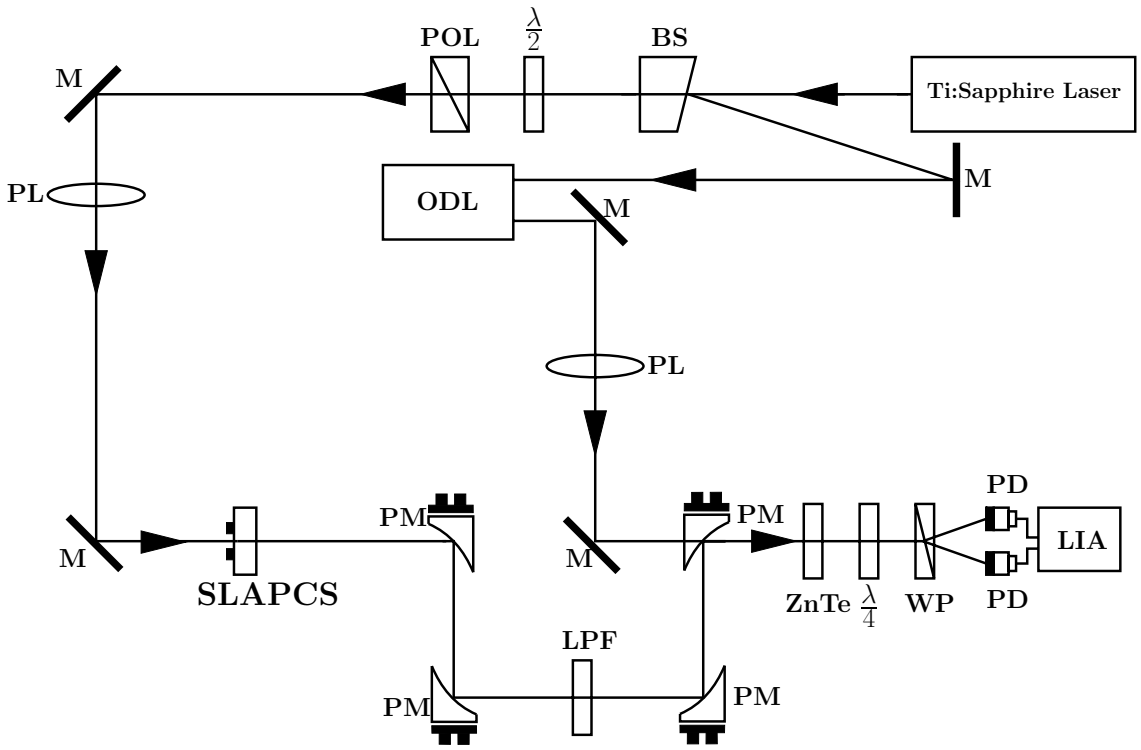

Fig. 1. Schematic diagram of the set-up. BS is a beam splitter; $\lambda/2$ is a half-wave plate; POL is a polarizer; M is a mirror; ODL is an optical delay line; PL is a positive lens, PM is a parabolic mirror; LPF is a low-pass filter blocking the optical leakage and passing the far-infrared radiation; $\lambda/4$ is a quarter-wave plate; WP is Wollaston prism; PD are photo-diodes; LIA is a lock-in-amplifier.

3. Birefringence of spruce

Birefringence is a very interesting phenomenon in single cycle radiation when viewed directly on a short time-scale with pulsed radiation in the time domain. The birefringence of an 8.3 mm thick piece of solid spruce wood was observed directly in the time domain by inserting the sample into the focal plane of the parabolic mirror system at the position of the low pass filter in Fig. 1. The measured transmission of the terahertz radiation is shown in Fig. 2.

The time-domain waveforms of transmitted terahertz radiation are examined as function of the orientation of the grain with respect to the terahertz polarization by rotating the wood sample. The angular dependence of the transmitted THz field is shown in Fig. 2 with the detection set to detect horizontally polarized transmitted terahertz radiation.

If the birefringent material is made sufficiently long, and the pulse-width of the electromagnetic radiation sufficiently short, then the effect of the birefringence will not only introduce a phase shift between orthogonal polarization components, but it also will introduce a propagation delay. Specifically, if the phase difference corresponds to a time-scale longer than the pulsewidth of the radiation, two orthogonally polarized pulses of electromagnetic radiation will result, the magnitude of which will depend on the orientation of the input polarization and the birefringent axes. When the angle between the input terahertz polarization and the visible grain is approximately 22^o, as seen in Fig. 2, the output radiation is comprised of two pulses, roughly equal in amplitude, and separated by approximately 2

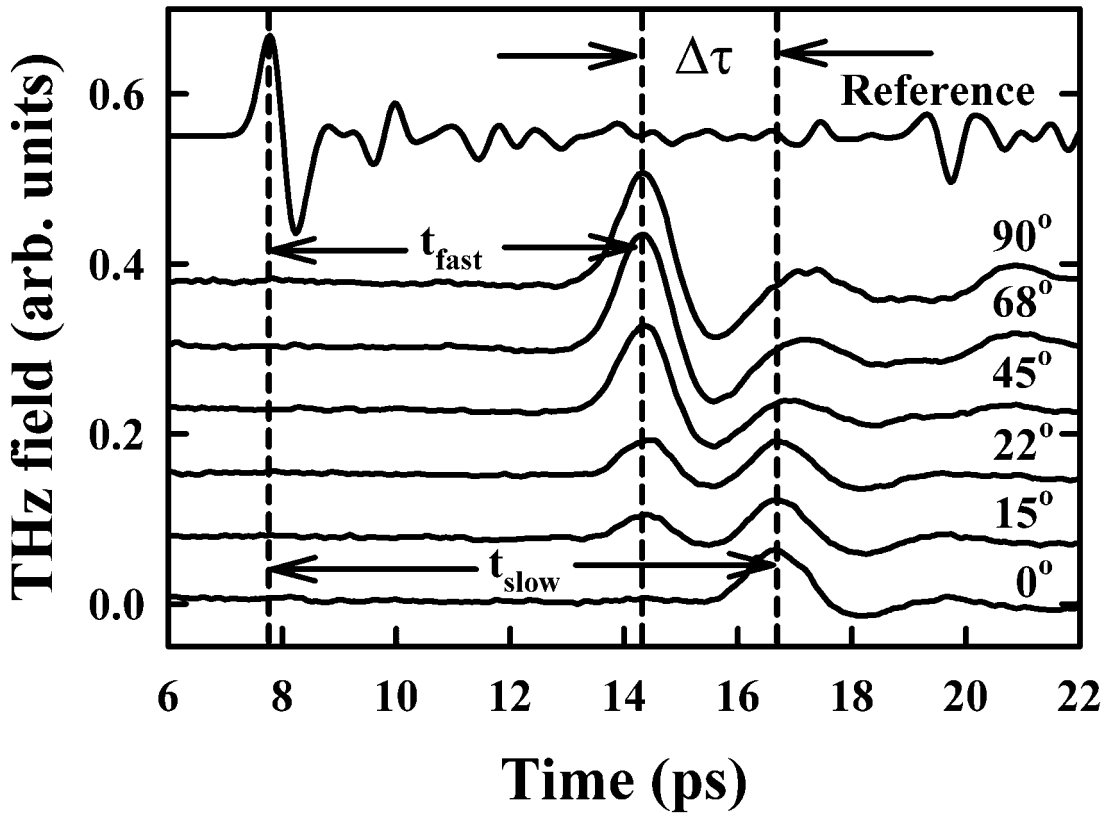

Fig. 2. Reference (top) and transmitted terahertz time-domain waveforms transmitted through an 8.3 mm piece of spruce wood is measured with the terahertz polarization making an angle θ with respect to the visible grain direction. Each scan is labeled by the corresponding value of θ used in the measurement, and the scans are offset for clarity. t_{fast} and t_{slow} indicate the time delay for propagation with terahertz polarization perpendicular and parallel to the visible grain, leading to fast and slow axes, respectively. $\Delta\tau$ is the time difference between terahertz propagation polarized parallel and perpendicular to the grain.

ps in time with orthogonal polarizations. The fact that the pulses have roughly equal amplitudes at an angle different than 45^o is a consequence of the diattenuation present within the wood, and will be discussed later in this report.

Based on the observed time delay between pulses of terahertz radiation propagating parallel and perpendicular to the visible grain, an estimate for the frequency averaged birefringence can be obtained directly from the time-domain data of Fig. 2. Assuming the birefringence is frequency independent, then the average birefringence, Δn, over the bandwidth of the transmitted terahertz pulse is related to the time delay between propagation with polarization parallel and perpendicular to the grain, $\Delta\tau$, by the relation:

$$\Delta n = \frac{c\Delta\tau}{L} \tag{1}$$

where c is the speed of light in vacuum and L is the thickness of the wood.

We estimate $\Delta\tau = 2.2$ ps from Fig. 2 and using L = 8.3 mm, the frequency averaged birefringence given by Eq. 1 is $\Delta n = 0.08 \pm 0.01$.

As the terahertz radiation is pulsed, and composed of a broad frequency spectrum, a more precise way to analyze the birefringence is to examine the index of refraction, which can be obtained from the transmitted spectrum. In fact, as the detection is coherent, we can extract the frequency-resolved complex index of refraction directly from the measured data. To do this, we use the thick sample approximation of Duvillaret et. al.,[14] truncating the time-domain spectrum before multiple reflections occur, and write the ratio of the measured

transmission spectrum to the reference spectrum as:

$$\frac{\vec{E}_{wood}(\nu)}{\vec{E}_{ref}(\nu)} = \hat{t}_{AW}\hat{t}_{WA}e^{-\frac{i2\pi\nu L}{c}(\hat{n}_W - \hat{n}_A)} \tag{2}$$

Where $\vec{E}_{wood}$ and $\vec{E}_{ref}$ are the measured terahertz fields in the frequency domain with and without wood in the beam paths, respectively, ν is the frequency, c is the speed of light in vacuum, L is the length of the wood sample, and $\hat{t}_{WA}$ and $\hat{t}_{AW}$ are the Fresnel transmission coefficients of wood-to-air and air-to-wood interfaces respectively. The Fresnel transmission coefficients are given by:

$$\hat{t}_{ij} = \frac{2\hat{n}_i}{\hat{n}_i + \hat{n}_j} \tag{3}$$

for normal incidence.[15] Writing the ratio of Eq. 2 in Euler form: $Re^{i\theta}$, we may make use of the measured data to extract the complex index $\hat{n}_W$. We take $\hat{n}_A$ = 1, and:

$$\hat{n}_W = n_W - ik_W \tag{4}$$

with the approximation in the Fresnel coefficients that $k \ll n$, to obtain:

$$Re^{i\theta} = \frac{\vec{E}_{wood}(\nu)}{\vec{E}_{ref}(\nu)} \approx \frac{4n_W}{(n_W+1)}e^{-\frac{2\pi\nu L}{c}k_w}e^{-\frac{i2\pi\nu L}{c}(n_w-1)} \tag{5}$$

Solving for n_W and k_W in Eq. 5, and using the relation $\alpha_W = 4\pi\nu k_W/c$ we obtain:

$$n_W = -\frac{\theta c}{2\pi\nu L} + 1 \quad (6)$$

$$\alpha_W = -\frac{2}{L} ln\left(R\frac{(n_W+1)^2}{4n_W}\right) \quad (7)$$

where α_W is the absorption coefficient.

In order to improve spectral resolution, a sample of spruce wood of thickness 3.025 mm was used to generate full frequency resolved transmission spectra. A reference scan was taken, as well as transmission scans with the terahertz polarization parallel and perpendicular to the visible grain. The reference and transmission data was Fourier transformed to the frequency domain, and Eq. 6 used to obtain the frequency-resolved index of refraction and absorption coefficient presented in Fig. 3. As clearly observed, the wood exhibits both birefringence and diattenuation.

A frequency averaged birefringence of 0.07 ± 0.006 is measured for the frequency range of 0.1 to 1.6 THz, in reasonable agreement with the time-domain estimate of 0.08 ± 0.01, given that different samples were used. The birefringence is also observed to be roughly frequency independent, indicating that the time-domain method of measuring the birefringence should be valid.

Since dry wood is not highly conductive, the difference in extinction for terahertz radiation propagating through the wood polarized parallel and perpendicular to the grain is possibly related to scattering. The cylindrical shape of the porous structures, which have diameters in the range of 80 to 140 μm for spruce wood,[16] may scatter more strongly

when the terahertz radiation is polarized parallel to the pores, in comparison to when it is polarized perpendicular to the pore axis. For a single long solid cylinder, the extinction coefficient is greater for polarization parallel to the cylinder axis, and the ratio of extinction coefficients ($Q_{ext}^{\parallel}/Q_{ext}^{\perp}$) grows with increasing frequency in the range of interest [1], similar to that observed in the present report.

Given that the index of refraction for these samples of solid wood are in the range of 1.25 - 1.35, the measured value for $\Delta n = 0.07 \pm 0.006$ is a large birefringence. This large birefringence is demonstrated by constructing waveplates in the far-infrared.

4. Investigation of waveplates constructed from spruce

We investigated the operation of a 3.025 mm thick piece of spruce as both a quarter- and half-waveplate for specific frequencies. First we computed what is expected for such devices when diattenuation is present. To do this, we calculate the angular dependence of the vertically and horizontally polarized terahertz fields after propagation through a 3.025 mm thick piece of spruce. Consider the geometry shown in Fig. 4.

The field at the output of the wood, parallel ($E_{\parallel}$) and perpendicular to the grain ($E_{\perp}$) structure is given by:

[1] For a long solid cylinder, with an index of refraction of 1.5, numerical calculations are shown in Fig. 67 of reference[17] for values of $0.1 < \rho < 1$, corresponding to a frequency range of 0.1-1 THz for a cylinder radius of 50 μm.

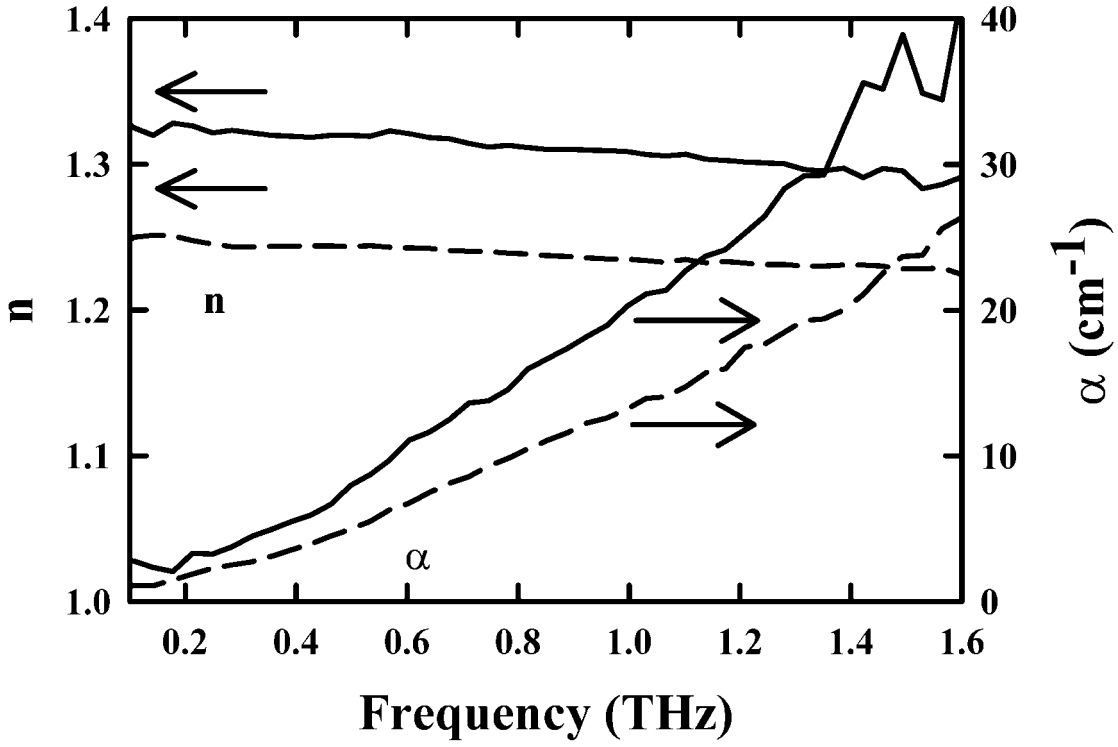

Fig. 3. Frequency resolved index of refraction (n) and absorption coefficient (α) obtained in transmission spectroscopy of a 3.025 mm thick piece of spruce wood. Measurements are taken with the terahertz polarization parallel to the grain (solid curves) and perpendicular to the grain (dashed curves).

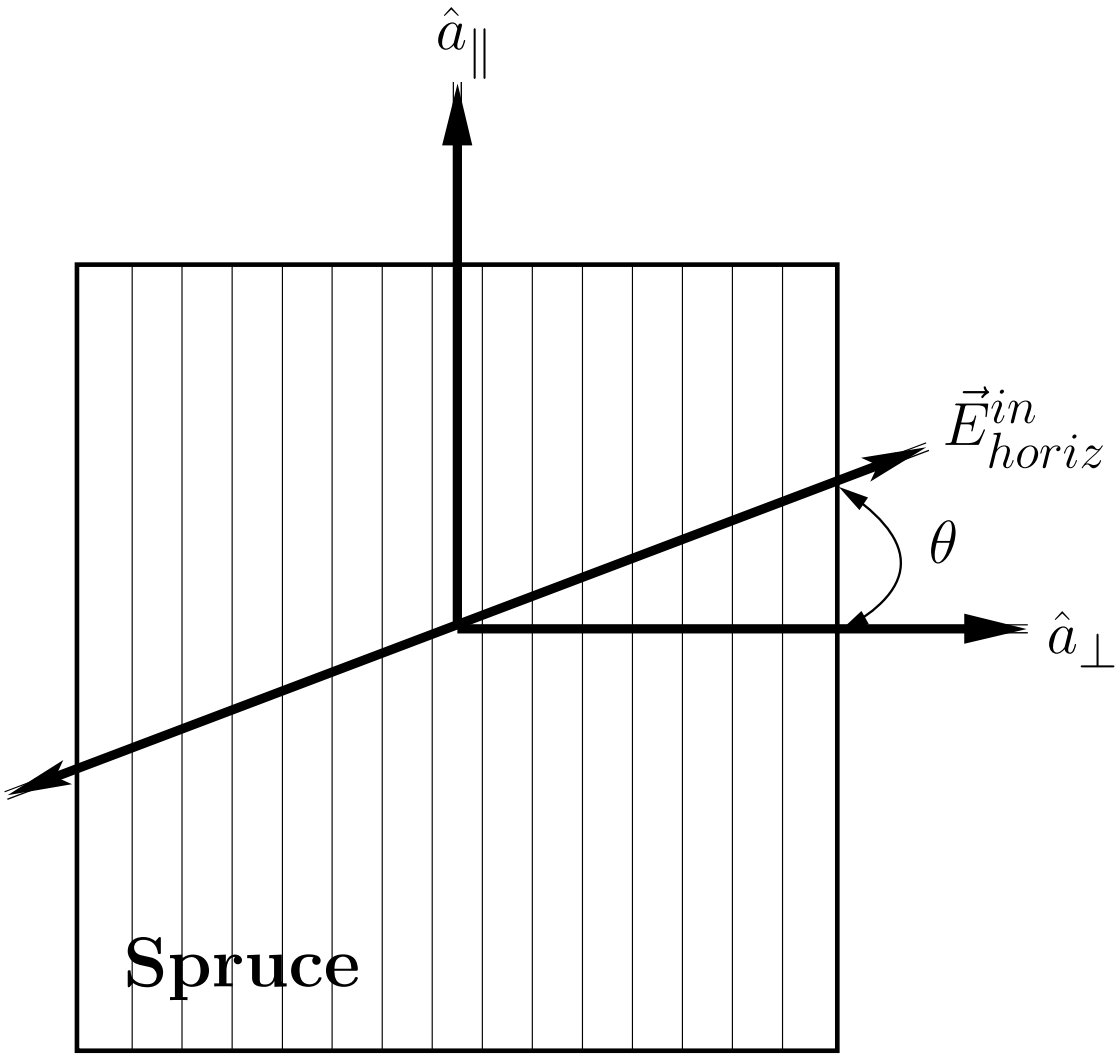

Fig. 4. Schematic diagram of the orientation of the wood with respect to analyzer axes (vertical and horizontal) for the input terahertz fields. The directions $\hat{a}_{\parallel}$ and $\hat{a}_{\perp}$ are parallel and perpendicular to the wood grain, respectively.

$$
\begin{aligned}
E_{\perp}^{out} &= E_{in}\cos(\theta)e^{i\Gamma_{\perp}}e^{-\frac{1}{2}\alpha_{\perp}d} \\
E_{\parallel}^{out} &= E_{in}\sin(\theta)e^{i\Gamma_{\parallel}}e^{-\frac{1}{2}\alpha_{\parallel}d}
\end{aligned}
\tag{8}
$$

where E_{in} is the incident electric field amplitude, θ is as defined in Fig. 4, $\Gamma_{\parallel}$ and $\Gamma_{\perp}$ are the incurred phase retardances along the grain and perpendicular to the grain, respectively, d is the thickness of the wood sample, and $\alpha_{\parallel}$ and $\alpha_{\perp}$ are the power absorption coefficients parallel and perpendicular to the grain, respectively.

In Fig. 4, the output fields along the two grain axes will recombine to form horizontally and vertically polarized THz fields at the output, to which our analyzer is sensitive. The vertical and horizontal components are given by:

$$
\begin{aligned}
E_{vert}^{out} &= E_{\parallel}^{out}\cos(\theta) - E_{\perp}^{out}\sin(\theta) \\
E_{horiz}^{out} &= E_{\perp}^{out}\cos(\theta) + E_{\parallel}^{out}\sin(\theta)
\end{aligned}
\tag{9}
$$

Using Eq. 8 in Eq. 9 we obtain the angular dependence of the magnitude of the horizontal and vertical components of the output field along the analyzer axes:

$$
\begin{aligned}
|E_{vert}^{out}| &= |E_{in}|e^{-\frac{1}{2}\alpha_{\parallel}d}|\sin(\theta)\cos(\theta)||1 - e^{i\Delta\Gamma}e^{-\Delta\alpha d}| \\
|E_{horiz}^{out}| &= |E_{in}|e^{-\frac{1}{2}\alpha_{\parallel}d}|\cos^2(\theta)e^{-\Delta\alpha d}e^{i\Delta\Gamma} + \sin^2(\theta)|
\end{aligned}
\tag{10}
$$

where $\Delta\alpha = \frac{1}{2}\left(\alpha_\perp - \alpha_\parallel\right)$ and $\Delta\Gamma = \Gamma_\perp - \Gamma_\parallel$ are the differences in absorption and induced phase for propagation along the grain and perpendicular to the grain, respectively.

Finally, taking Eq. 10 with $\Delta\Gamma = \frac{\pi}{2}$ and $\Delta\Gamma = \pi$, the expressions for the terahertz field magnitudes as a function of the angular orientation of the wood for quarter- and half-waveplate behaviour are obtained:

$$\begin{aligned}
E_{vert}^{out,QWP} &= E_{in}e^{-\frac{1}{2}\alpha_\parallel d}|\sin(\theta)\cos(\theta)|\sqrt{1+e^{-2\Delta\alpha}} \\
E_{vert}^{out,HWP} &= E_{in}e^{-\frac{1}{2}\alpha_\parallel d}|\sin(\theta)\cos(\theta)|\left(1+e^{-\Delta\alpha d}\right) \\
E_{horiz}^{out,QWP} &= E_{in}e^{-\frac{1}{2}\alpha_\parallel d}\sqrt{\sin^4(\theta)+\cos^4(\theta)e^{-2\Delta\alpha d}} \\
E_{horiz}^{out,HWP} &= E_{in}e^{-\frac{1}{2}\alpha_\parallel d}\sqrt{\left(\sin^2(\theta)(1+e^{-\Delta\alpha d})-e^{-\Delta\alpha d}\right)^2}
\end{aligned} \tag{11}$$

Note that only specific frequencies will meet the criteria for $\Delta\Gamma = \frac{\pi}{2}$ and $\Delta\Gamma = \pi$. We estimate the matching wavelength to the desired phase retardance and birefringence (Δn) to be:

$$\lambda_{match} = \frac{2\pi L}{\Delta\Gamma}\Delta n \tag{12}$$

where λ_{match} is the matching wavelength, Δn is the birefringence and $\Delta\Gamma$ is the desired phase retardance. From Fig. 3, we have an approximately frequency independent birefringence of $\Delta n = 0.07 \pm 0.006$, which gives a matching wavelength of 847 μm (or 0.35 THz) and 424 μm (or 0.71 THz) for quarter-wave ($\Delta\Gamma = \pi/2$) and half-wave ($\Delta\Gamma = \pi$) phase

retardance, respectively, for a 3.025 mm thick piece of spruce.

Taking terahertz time-domain scans as a function of the angle θ in Fig. 4, and Fourier transforming to the frequency domain, a set of frequency spectra is obtained. The amplitudes in specific frequency bins, with a width of 40 GHz, are computed to form an angularly resolved measurement for each frequency bin. Both horizontally polarized and vertically polarized transmitted terahertz fields are measured in this way. The result is plotted for a frequency bin centered at 0.356 THz in Fig. 5. The solid lines are expected for the birefringence as given by Eq. 11.

A similar result is obtained for operation as a half-wave plate. In this case, the best fit to the data is for the 0.71 THz frequency bin, as expected based on the matching wavelength calculated above. The angularly resolved s- and p-polarized transmitted fields at 0.71 THz are plotted in Fig. 6 together with the predicted output using Eq. 11.

These results clearly demonstrate the behavior of spruce as a waveplate for frequencies in the far infrared. While likely not a practical device due to significant attenuation within the wood, the possibility for constructing birefringent elements from wood is clearly demonstrated.

5. fibre-orientation analysis using terahertz time-domain spectroscopy

Paper products are a derivative of wood, and therefore contain wood fibre. The fibre of the wood is what leads to the birefringence that was demonstrated earlier. Therefore, depending on whether or not there exists a preferential orientation of the fibres within a paper product,

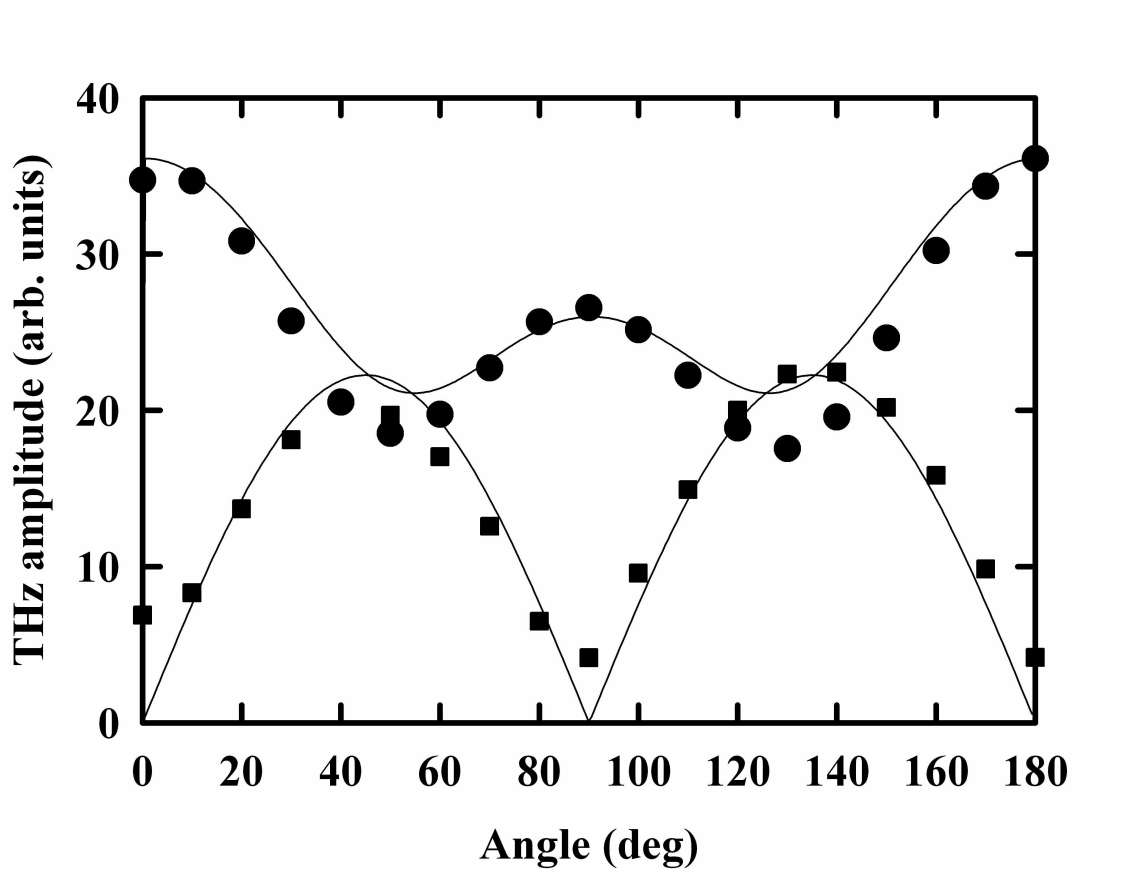

Fig. 5. Measured THz transmission for the 365 GHz frequency bin data as a function of wood orientation . The data for vertically (squares) and horizontally (circles) polarized terahertz fields are shown for transmission through 3.025mm thick spruce, along with the expected angular dependence for behavior as a quarter-wave plate (Eq. 11. The angle is defined as the angle that the grain direction makes with the vertical axis.

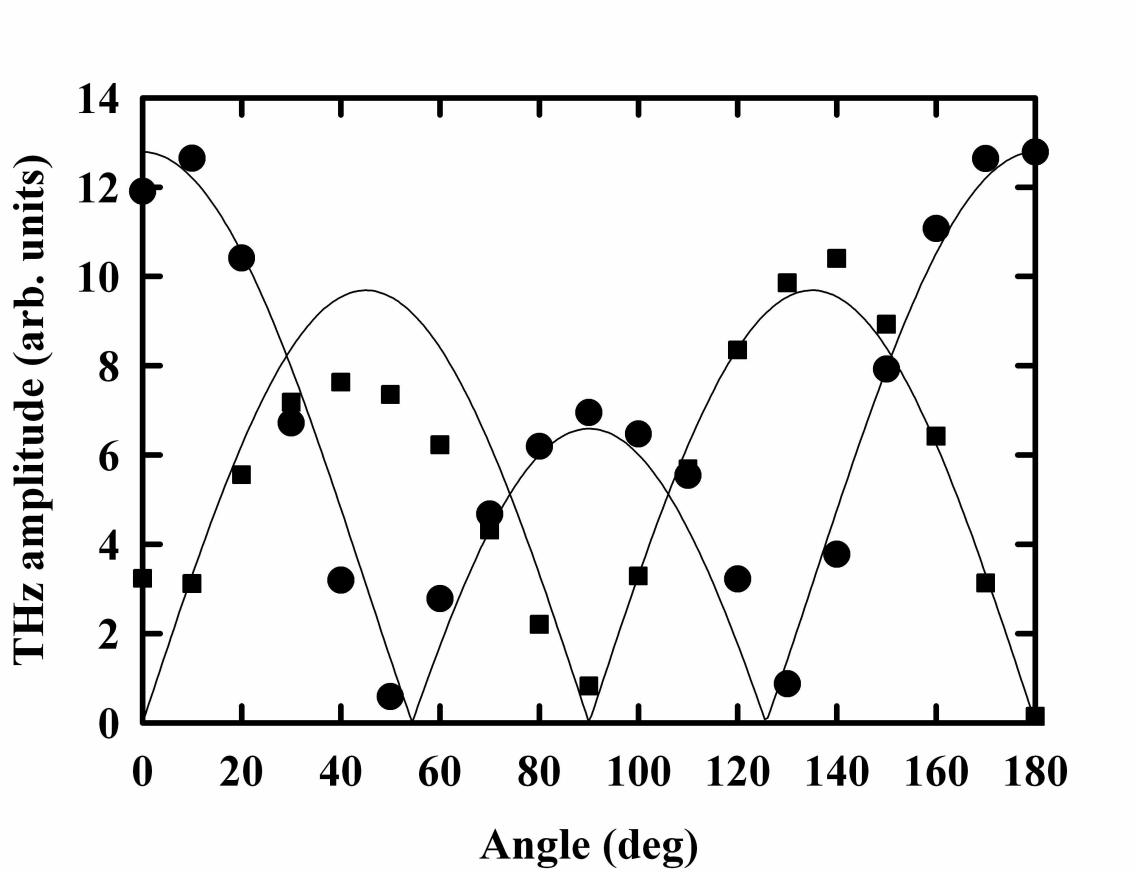

Fig. 6. THz transmission for the 711 GHz frequency bin data as a function of wood orientation. The data for vertically (squares) and horizontally (circles) polarized terahertz fields are shown for transmission through 3.025mm thick spruce, along with the expected angular dependence for behavior as a half-wave plate (Eq. 11). The angle is defined as the angle that the grain direction makes with the vertical axis.

one might expect paper to also exhibit birefringence. Lens paper is a typical example of such a product and it is easily verified that lens paper has a preferential fibre orientation. This is most easily observed by tearing the paper. One will find that the paper preferentially tears along one fixed direction, while it is difficult to tear the paper in any other direction.

The birefringence associated with this fibre orientation is easily verified. A collection of 27 pieces of identically oriented lens paper was put in the terahertz spectrometer set-up. It was immediately observed that the position of the maxima of the terahertz pulse in the time domain changed as a function of the orientation of the lens paper with respect to the polarization of the terahertz beam. This is the time-domain manifestation of birefringence outlined earlier.

In fact, the orientation of the fibres with respect to the polarization of the terahertz beam is easily mapped out using the change in time-delay as a function of the orientation of the lens paper. Consider that the index of refraction is $n_\perp$ and $n_\parallel$ when the polarization of the terahertz radiation is perpendicular and parallel to the preferential fibre orientation, respectively, and the 27 pieces of lens paper form a sample of thickness d_{lens}. Then the time delay, $\Delta\tau$, as a function of the orientation of the lens paper with respect to the terahertz polarization is given by:

$$\Delta\tau = \frac{d_{lens}}{c}\left[n_\perp \cos(\theta) + n_\parallel \sin(\theta)\right] \tag{13}$$

where c is the speed of light in vacuum, θ is the angle that the linear polarization of the

terahertz radiation makes with the vector perpendicular to the fibre orientation, and the quantity in braces is the effective index of refraction for propagation through the lens paper at normal incidence for this polarization state.

This time delay is most easily measured on a portion of the terahertz time-domain waveform that is rapidly changing in time. Therefore, we choose a rapidly varying linear portion of the terahertz time-domain waveform as the operating point as shown in Fig. 7.

Once the optical delay-line is fixed at the operating point shown in Fig. 7, the signal on the lock-in amplifier is zeroed. The resultant change in signal as the orientation of the lens paper is changed is a direct measure of $\Delta\tau$. The result is plotted in Fig. 8.

The lock-in amplifier signal (time-delay) is negative in Fig. 8 as the angle is defined as the angle that the linearly polarized terahertz beam makes with the fibre orientation. Since the fibre axis is the slow-axis, as the angle is rotated by 90 degrees ($E_{THz} \parallel n_{\perp}$), it falls along the fast-axis and therefore arrives earlier leading to negative time-delays and a decrease in signal due to the operating point chosen. Once the data is taken over an angular range of 90 degrees, it is then possible to determine the orientation of the polarization with respect to the preferential fibre alignment at an arbitrary position.

The important point for a practical application is that the full terahertz time-domain waveform is unnecessary. A simple measurement of a relative lock-in amplifier signal (time-delay) is sufficient once the indeces of refraction are known and the operating point chosen.

Another important point for practical applications is that the time required to obtain data

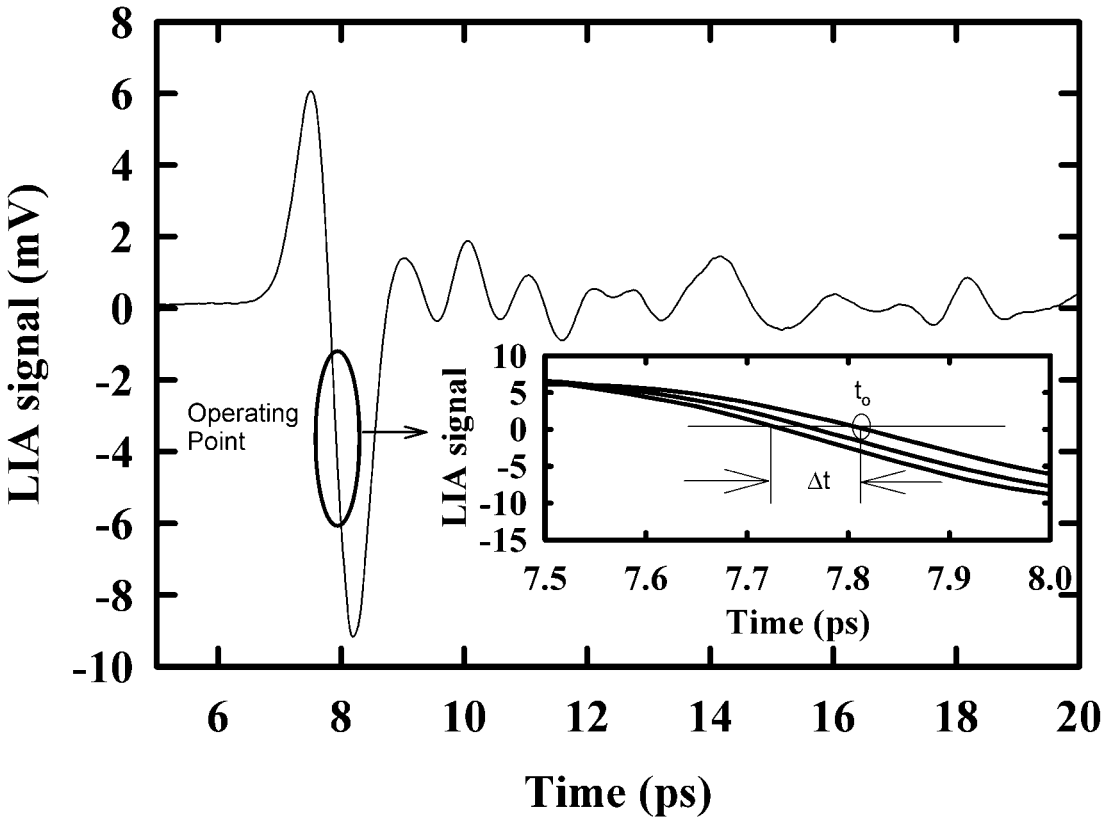

Fig. 7. Operating point for mapping time delay of terahertz radiation to birefringence data. The figure shows a typical terahertz time-domain waveform, and the orientation of the operating point is shown in the inset. The lock-in amplifier signal is zeroed at the operating point, and the lens paper sample is rotated about it's surface normal to map time-delay to amplitude information.

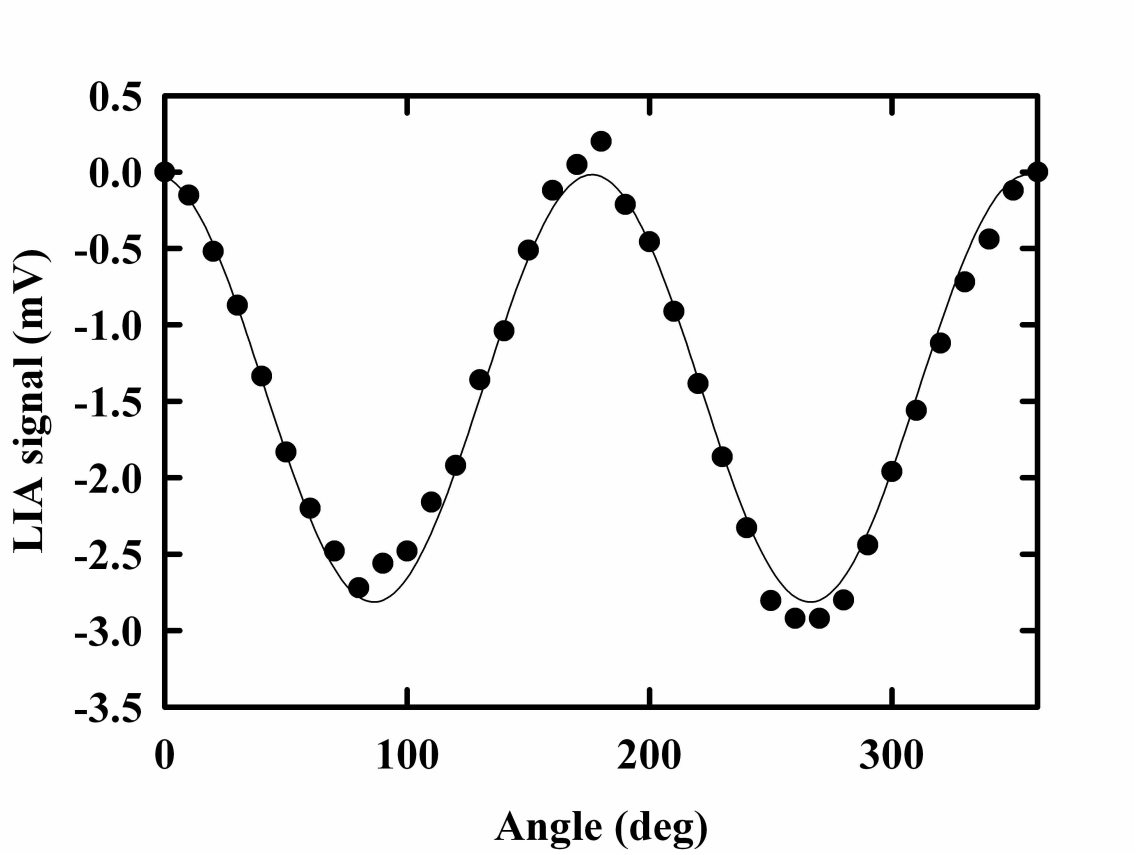

Fig. 8. Lock-in amplifier signal as a function of orientation for transmission of terahertz radiation through 27 pieces of aligned lens paper. The lens paper oriented with fibre alignment vertical corresponds to zero degrees in the figure. The input terahertz field is polarized horizontally. The measured signal corresponds to mapping time delay to birefringence (see text for details).

over a 90 degree span is essentially limited by the lock-in time constant. In this case a lock-in amplifier time constant of 100 ms was used, such that a 90 degree scan could take a fraction of a second.

Finally, a single piece of lens paper, $21\mu m$ thick, was measured using a terahertz time-domain waveform acquired in 3 seconds, limited by the speed of the optical delay line, for each polarization orientation. A reference scan is taken, and then a transmission scan with the terahertz polarization parallel and perpendicular to the grain. The complete frequency-resolved measurement of the indeces of refraction is computed, and the data presented in Fig. 9.

The frequency-resolved index measurements of the single piece of lens paper demonstrate the birefringence is quite large in the lens paper, with a frequency-averaged value of $\Delta n = 0.10 \pm 0.03$ in the frequency range of 0.2 - 1.4 THz. The data is fairly noisy as a consequence of the short time scan for the transmission measurements, and the fact that the reference and transmitted signals are only very slightly different.

6. Conclusion

It was demonstrated that solid spruce wood is birefringent, with a birefringence of 0.07 $\pm$ 0.006, which is approximately frequency independent in the range of 0.1 to 1.6 THz. The extinction coefficient was shown to depend on the terahertz polarization, and therefore exhibits diattenuation. The birefringence was investigated in detail for quarter- and half-waveplate configurations centered at 0.36 and 0.72 THz, respectively, showing more

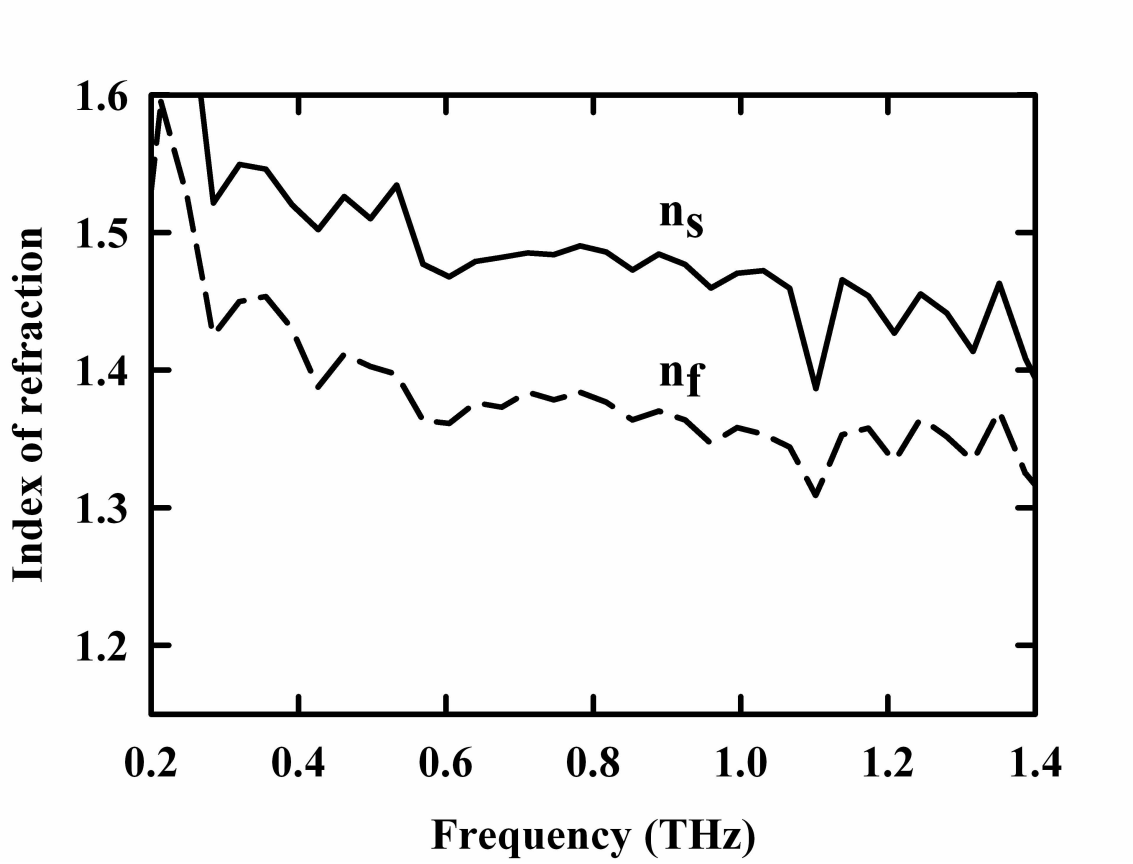

Fig. 9. Index of refraction of a 21 μm thick piece of lens paper obtained with terahertz polarization perpendicular (long dashed) and parallel (solid) to the fibre orientation. n_f and n_s represent the fast and slow axes, respectively.

complex behaviours due to the diattenuation. The fibre alignment in standard laboratory lens paper was also measured using THz radiation and served to demonstrate the possibility of using pulsed terahertz radiation for fibre orientation analysis of single sheets of lens tissue.

This work was supported by MPB Technologies Inc. and NSERC. One of the authors (MR) would like to acknowledge partial financial support provided by iCORE.

References

1. G. C. Walker, E. Berry, N. N. Zinov'ev, A. J. Fitzgerald, R. E. Miles, M. Chamberlain, and M. A. Smith, "Teraherz imaging and international safety guidelines," in *Proc. SPIE*, vol. 4682, pp. 683–690, 2002.
2. D. M. Mittleman, M. Gupta, R. Neelamani, R. G. Baraniuk, J. V. Rudd, and M. Koch, "Recent advances in terahertz imaging," *Appl. Phys. B*, vol. 68, pp. 1085–1094, 1999.
3. M. C. Kemp, P. F. Taday, B. E. Cole, J. A. Cluff, A. J. Fitzgerald, and W. R. Tribe, "Security applications of terahertz imaging," in *Proc. SPIE*, vol. 5070, pp. 44–52, 2003.
4. W. R. Tribe, D. A. Newnham, P. F. Taday, and M. C. Kemp, "Hidden object detection: security applications of terahertz technology," in *Proc. SPIE*, vol. 5354, pp. 168–176, 2004.
5. M. Koch, S. Hunsche, P. Schaucher, M. C. Nuss, J. Feldmann, and J. Fromm, "THz-imaging: a new method for density mapping of wood," *Wood Sci. Technol.*, vol. 32, pp. 421–427, 1998.

6. S. Hunsche and M. C. Nuss, “Terahertz ”T-ray” tomography,” in *Proc. SPIE*, vol. 3465, pp. 426–433, 1998.

7. Y. W. Lim, A. Sarko, and R. H. Marchessault, “Light scattering by cellulose II. Oriented condesned paper,” *TAPPI J.*, vol. 53, pp. 2314–2319, 1970.

8. P. H. Friedlander, “The measurement of fibre orientation in newsprint with respect to the machine direction by X-ray diffraction,” *Pulp and Paper Magazine of Canada*, vol. January, pp. 102–103, 1958.

9. H. Ruck and H. Krässig, “The determination of fibre orientation in paper,” *Pulp and Paper Magazine of Canada*, vol. June, pp. 183–190, 1958.

10. C. M. Crosby, A. R. K. Eusufazi, R. E. Mark, R. W. Perkins, J. S. Chang, and N. V. Uplekar, “A digitizing system for quantitative measurement of structural parameters in paper,” *TAPPI J.*, vol. 64, pp. 103–106, 1981.

11. M. Reid and R. Fedosejevs, “Quantitative comparison of THz emission from (100) InAs surfaces and GaAs large-aperture photoconductive switch at high fluences,” *Appl. Opt.*, vol. 44, pp. 149–153, 2004.

12. G. Zhao, R. N. Schouten, N. van der Valk, W. T. Wenckebach, and P. C. M. Planken, “Design and performance of THz emission and detection setup based on a semi-insulating GaAs emitter,” *Rev. Sci. Inst.*, vol. 73, pp. 1715–1719, 2002.

13. P. C. M. Planken, H.-K. Nienhuys, H. J. Bakker, and T. Wenckebach, “Measurement and calculation of the orientation dependence of terahertz pulse detection in ZnTe,” *J.*

Opt. Soc. Am. B., vol. 18, pp. 313–317, 2001.

14. L. Duvillaret, F. Garet, and J.-L. Coutaz, "A reliable method for extraction of material parameters in terahetz time-domain spectroscopy," *IEEE J. Sel. Top. Quant.*, vol. 2, pp. 739–746, 1996.
15. J. D. Jackson, *Classical Electrodynamics*. New York: John Wiley and Sons, Inc., 3rd ed., 1999.
16. A. J. Stamm, *Wood and Cellulose Science*. New York: The Ronald Press Company, 1st ed., 1964.
17. H. C. van de Hulst, *Light Scattering by Small Particles*. New York: Dover Publications, 1st ed., 1981.